Analysis of Radar Micro-Doppler Signatures From Experimental Helicopter and Human Data

Thayananthan Thayaparan, Sumeet Abrol, Edwin Riseborough, LJubiša Stankovic, Denis Lamothe, Grant Duff

Abstract—**This paper highlights the extraction of micro-Doppler (m-D) features from radar signal returns of helicopter and human targets using the wavelet transform method incorporated with time-frequency analysis. In order for the extraction of m-D features to be realized, the time domain radar signal is decomposed into a set of components that are represented at different wavelet scales. The components are then reconstructed by applying the inverse wavelet transform. After the separation of m-D features from the target's original radar return, time-frequency analysis is then used to estimate the target's motion parameters. The autocorrelation of the time sequence data is also used to measure motion parameters such as the vibration/rotation rate. The findings show that the results have higher precision after the m-D extraction rather than before it, since only the vibrational/rotational components are employed. This proposed method of m-D extraction has been successfully applied to helicopter and human data.**

I. Introduction

When a radar transmits an electromagnetic signal to a target, the signal interacts with the target and then returns to the radar. Any changes in the properties of the returned signal are generally due to its interaction with the target. This being the case, the characteristics of the target in question are reflected in the returned signal, and it follows that various properties of the target can be extracted from the returned signal. For example, when the target is moving, the carrier frequency of the returned signal will be shifted due to the Doppler effect. This Doppler frequency shift can then be used to determine the radial velocity of the moving target.

IEE Proc. Radar, Sonar and Navigation,, Vol. 1, No. 4, Aug. 2007

It frequently occurs that a target or some structure on the target is vibrating or rotating in addition to the target's translation. These vibrations and rotations are referred to as micro-motion dynamics [1-7]. The micro-motion dynamics of a target generate frequency modulations of the returned signal in addition to the Doppler frequency shift caused by the target's translational motion. In fact, the frequency modulations of the returned signal induced by the micro-motions produce sidebands about the target's Doppler frequency. The frequency modulation due to micro-motion dynamics is called the micro-Doppler (m-D) phenomenon [1-7].

While the Doppler frequency shift created by the translational motion of the target is time-invariant at a constant velocity, the Doppler frequency shift generated by micro-motion dynamics is a time-varying function that imposes a periodic time-varying modulation onto the carrier frequency. The modulation contains harmonic frequencies that depend on the carrier frequency, the vibration or rotation rate, and the angle between the direction of vibration and the direction of the radar's incident wave.

The m-D phenomenon is of interest because information regarding a target's micro-motion dynamics is preserved in the returned radar signal. The m-D phenomenon is commonly encountered in radar returns because real world targets (e.g., helicopter, vehicle, rotating antenna) are usually engaged in complicated manoeuvres that incorporate translation, vibrational and rotational motions. The mechanical vibration/rotation of a target or part of the target's structure appears in a radar image as smeared features and induces frequency modulation on radar returns [1-11]. On the other hand, m-D features could provide distinctive information for recognition of targets of interest. They have been used to identify the natural resonant frequency of a tractor-trailer truck [8]. The m-D features of the Jet Engine Modulation (JEM) lines in a Mi-24 Hind-D helicopter are also used to estimate the turbine rotation rate and the number of turbine blades [9].

One of the problems with helicopter identification using JEM signatures is the complexity of the signal [12]. Due to this complexity, its exact nature is difficult to define. This requires more refined signal processing techniques in order to extract the relevant information from background noise, clutter and extraneous harmonics. Traditional spectral analysis techniques have been developed, however, the signal-processing task is often complicated by a low signal-to-noise ratio (SNR) and the presence of spurious spectral lines introduced by the radar. Traditional analyses, such as Fourier analysis or the sliding window FFT (short time Fourier transform), lack the necessary resolution for extracting and processing these unique features. Therefore, high-resolution analysis is necessary for analyzing m-D information. Promising alternatives for these cases are techniques that are based on time-frequency analysis methods [1-7].

Obtaining radar signatures of personnel is another important application of m-D. The human walking gait is a complex motion behavior that comprises different movements of individual body parts. Since September 11, 2001, Automatic Gait Recognition (AGR) technology has grown in significance. Because gait recognition technology is so new, researchers are assessing its uniqueness and methods by which it can be evaluated. Various computer vision and ultrasound techniques have been developed to measure gait parameters [13-18]. Real-Time AGR radar systems have recently been recognized as advantageous solutions for detecting, classifying and identifying human targets at distances in all light and weather conditions. Radar has certain advantages over electro-optical (EO) systems and video cameras in that it can penetrate clothes, does not require light, and operates in fog and other low-visibility weather conditions. However, radar-based recognition is such a new approach that much fundamental research has yet to be done in this area. The radar sends out a signal and then measures the echo that contains rich information about the various parts of the moving body. There are different shifts for different body parts, because they are moving at different velocities. For example, a walking man with swinging arms may induce frequency modulation of the returned signal and generate sidebands about the body Doppler. In this paper, we develop the preliminary ground work for this challenging field of research.

It is reasonable to expect that the m-D features representing the micro-motions of a target can be extracted from the returned signal, much in the same way as properties are extracted from radar returns of targets undergoing only translational motion. Since different targets produce different micro-motions, every target would have its own "m-D signature", making it possible to distinguish and identify targets under consideration based on the additional information provided by the m-D features. Hence, an effective method is needed for extracting m-D features in order to fully exploit the additional and unique information they provide.

Although there have been studies of micro-Doppler effects in radar in the past few years [1-7], there are only a few experimental trials performed so far that are specifically dedicated to helicopter and human micro-Doppler research. As such, this paper contributes additional experimental micro-Doppler data and analysis which should help in developing a better picture of the micro-Doppler effect in radar in the future. Furthermore, instead of using the conventional Fourier transform or the high-resolution time-frequency transform alone, as was done in the past [1-7], the wavelet transform method combined with time-frequency analysis is used in this paper to analyze the time-varying micro-Doppler features. Section 2 briefly provides an introduction to the basic mathematical description of the m-D phenomenon. Section 3 discusses the method of m-D feature extraction, which is based on wavelet digital filter banks and time-frequency methods. Results are presented in Section 4 and show that m-D features can be accurately extracted using the wavelet transform method. The motion parameters are estimated with the time-frequency analysis and autocorrelation techniques. Conclusions and recommendations for future studies are given in Section 5.

II. Basic Mathematical Description of the Micro-Doppler Phenomenon

The basic mathematical description of the m-D phenomenon induced by vibrational motions is discussed in this section. Rotation can be seen as a special case of vibration. In coherent radar, the variations in range cause a phase change in the returned signal from a target. A half-wavelength change in range can cause 360-degree phase change. It is conceivable that the vibration of a reflecting surface may be measured with the phase change. Thus, the Doppler frequency shift that represents the change of phase function with time can be used to detect vibrations or rotations of structures in a target [1]. Mathematics of the m-D effect can be derived by introducing vibration or rotation (micro-motion) to the conventional Doppler analysis. A target can be represented as a set of point scatterers, which are the primary reflecting points on the target. The point scattering model can simplify the analysis while preserving the m-D induced by micro-motions. In our case, there exists a vibrating point scatterer in a returned radar signal. The received Doppler from a target as a function of time is modeled by the following equation

$$s(t) = Ae^{(j(2\pi f_0 t + \phi(t)))}, \tag{1}$$

where A is the reflectivity of the vibrating point scatterer and f_0 is the carrier frequency of the transmitted signal. The $\phi(t)$ is the time-varying phase change of the vibrating scatterer. Assuming that the vibrating scatterer is set to a radian frequency oscillation of ω_ν , the time-varying phase is

$$\phi(t) = \beta \sin(\omega_\nu), \tag{2}$$

where $\beta = 4\pi D_\nu/\lambda$, D_ν is amplitude of the vibration and λ is the wavelength of the transmitted signal [3]. Substituting eq. (2) into eq. (1) yields

$$s(t) = Ae^{(j(2\pi f_0 t + \beta \sin(\omega_\nu t)))}. \tag{3}$$

Equation (3) may be written in a Fourier series expansion as follows

$$s(t) = A \sum_{n=-\infty}^{\infty} c_n e^{j(2\pi f_0 + n\omega_\nu)t}. \tag{4}$$

The Fourier coefficient c_n will be expressed as

$$c_n = \frac{1}{2\pi} \int_{-\pi}^{\pi} e^{j\beta \sin \omega_\nu t} e^{-jn\omega_\nu t} dt = J_n(\beta), \tag{5}$$

which is an nth-order Bessel function of the first kind [5]. Substituting eq. (5) into (3) yields

$$s(t) = A \sum_{n=-\infty}^{\infty} J_n(\beta) e^{(j(2\pi f_0 + n\omega_\nu)t)}. \tag{6}$$

Equation (6) shows a m-D frequency spectrum that consists of pairs of harmonic spectral lines around the center frequency f_0. The spacing between adjacent spectral lines is $\omega_\nu/2\pi$. Furthermore, since the phase term function in eq. (3) is time varying, the instantaneous frequency f_D, i.e. the m-D frequency induced by the vibration of the scatterer, may be expressed as

$$f_D = \frac{1}{2\pi}\frac{d\phi}{dt} = \frac{1}{2\pi}\beta\omega_\nu \cos(\omega_\nu t) = \\ = \frac{2}{\lambda} D_\nu \omega_\nu \cos(\omega_\nu t). \tag{7}$$

Note that the maximum m-D frequency change is $(2/\lambda)D_\nu\omega_\nu$, which is used to estimate the displacement of a vibrating scatterer. The m-D induced by vibration is a sinusoidal function of time at the vibrating frequency ω_ν. Usually, when the vibrating modulation is small, it is difficult to detect the vibration in the frequency domain. Thus, a method that is able to separate the radar return induced by the target body from that induced by its vibrating structure might help to isolate the vibrating spectrum from other contributions.

This new technology can be developed for m-D applications of military significance (e.g., helicopter rotors, aircraft propellers, JEM of an air target, rotating ship or aircraft antennas, human walking gait analysis, vibrations of a vehicle/tank, etc.).

Modulation induced by rotating structures can be regarded as a unique signature of a target. This m-D signature is an important feature for identifying targets of interest (i.e. helicopters, ships or aircraft with rotating antennas). When there is a rotating scatterer on a target, the phase term in eq. (2) may be expanded as follows

$$\phi(t) = \beta \sin(\Omega t + \theta_0), \tag{8}$$

where Ω is the rotation rate and θ_0 is the rotating angle of the scatterer on the rotating structure at $t = 0$, called initial rotating angle. Therefore, the received Doppler from one rotating scatterer may be expressed by eq. (9), which is an expansion of a vibrating structure, i.e.

$$s(t) = Ae^{(j(2\pi f_0 t + \beta \sin(\Omega t + \theta_0)))}. \tag{9}$$

Equation (9) may also be expressed by the Bessel function of the first kind. Similar to eq. (6), m-D consists of harmonic spectral lines around the center frequency. If there are N rotating scatterers on a target (such as the rotor blades of a helicopter), there will be N different initial rotating angles, i.e.

$$\theta_k = \theta_0 + k2\pi/N, \tag{10}$$

for $k = 0, ..., N-1$; and thus the total received signal becomes

$$s(t) = \sum_{k=0}^{N-1} Ae^{(j(2\pi f_0 t + \beta \sin(\Omega t + \theta_0 + k2\pi/N)))}. \tag{11}$$

A detailed mathematical description of micro-Doppler modulations induced by several typical basic micro-motions is derived in [1,7]. This description is beyond the scope of this paper.

III. Method of Micro-Doppler Feature Extraction

The Fourier transform is the most common method to analyze the properties of a signal waveform in the frequency domain. However, due to lack of localized time information, the Fourier transform cannot provide more complicated time-varying frequency modulation information [19]. A joint time-frequency analysis that provides localized time-dependent frequency information is needed for extracting time-varying motion dynamic features [20-23]. To analyze the time-varying frequency characteristics of the micro-Doppler modulation and visualize the localized joint time and frequency information, the signal must be analyzed by using a high-resolution time-frequency transform, which characterizes the temporal and spectral behavior of the analyzed signal. For example, by examining the time information and the sign of the micro-Doppler shift caused by a movement, the direction of the movement at the specific time could be found.

Joint time-frequency analysis is the basis of most of the existing methods used to extract m-D features [1-7]. Another viable approach to extracting m-D features is wavelet analysis. The main motivation for applying wavelet analysis in the extraction of m-D features is that the micro-motion dynamics of a target that induce m-D features change at a rate much faster than the target itself. Wavelet analysis has the capability of detecting rapid changes of a signal [24-25]. Therefore, wavelet analysis seems ideal for the extraction of m-D features and the wavelet transform can be considered a powerful tool for this task.

The tree of digital filter banks for computing the discrete wavelet transform is given in Figure 1a (this is a four-level decomposition tree). L and H represent pairs of discrete low-pass and high-pass filters. As demonstrated in this figure, the original signal S is decomposed into its constituent parts consisting of cd_1, cd_2, cd_3, cd_4, and ca_4. In other words, after decomposition S = ca_4 + cd_1 + cd_2 + cd_3 + cd_4. Now, the wavelet transform has decomposed the signal into five parts; the four detail levels and the stationary approximation. Gen-

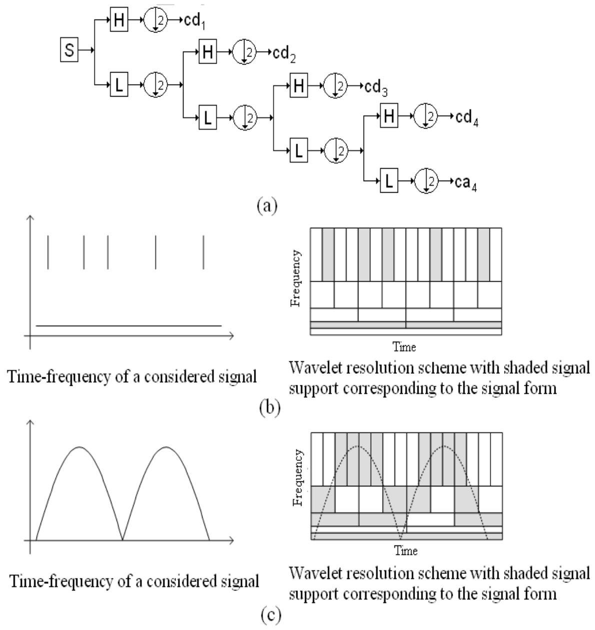

Fig. 1. (a) The tree of filter banks for computing the discrete wavelet transform; (b) time-frequency representation of a considered signal and its wavelet resolution scheme; (c) signal with sinusoidally frequency modulated component and its wavelet resolution scheme.

erally, these decomposed parts, by themselves, do not represent motion dynamics of the target in question. Depending on the physical quantity that one wishes to estimate, the decomposed parts of the signal may need to be combined in various ways in order to represent the m-D features for which motion parameters are required. After the comparison and evaluation of different wavelets [25], the results show that four-level decomposition and reconstruction with db1 wavelet is sufficient to extract m-D features in this study.

Now, let us consider a signal whose time-frequency description is given in Figure 1b. We can easily conclude that this signal is well suited for the wavelet analysis. Its high frequency components are short in time, while its low frequency components are of long duration. This is exactly as the standard wavelets require. Therefore, the application of the wavelets for its analysis and separation will produce good results, as in our experimental helicopter data. Let us now consider another signal, with a sinusoidally frequency modulated component as in Figure 1c. We can see that the wavelet scheme (on the right) does not fit the analysis for these kind of signals. This signal has short and fast crossings at the low frequencies (where the wavelet has very low time resolution) and the signal resolution at the high frequencies will be extremely low, which is not good for the analysis. Therefore, if we want to analyze the signals as in Figure 1b, the wavelets could be used with good results, but in the cases of FM signals over the entire frequency scale as in Figure 1c, the standard wavelets are not appropriate.

In this paper, we are not using the wavelet analysis alone, or the time-frequency analysis alone. Rather, we are using the wavelet analysis to separate the rotating part signal from the main body signal. The wavelet analysis considerably "cleans up" the signal. Thereafter, the time-frequency analysis is employed to analyze the oscillation and to estimate the motion parameters. There are many different time-frequency transforms that include linear transforms, such as the short-time

Fourier transform (STFT), and bilinear transforms, such as the Wigner-Ville distribution (WVD), available in the literature [1-7,20-23]. Each transform offers advantages and disadvantages. Certain transforms provide excellent resolution, but are slow to calculate. Others provide poor resolution, but are quick to calculate. Some transforms provide a good balance of speed and resolution, but have interference cross-terms. In principle, any time-frequency transform can be used to analyze the micro-Doppler modulation. However, a desired time-frequency transform should satisfy the requirements for high-resolution in both the time and frequency domains and low cross-term interference. After the comparison and evaluation of many different time-frequency transforms, we found that the smoothed pseudo Wigner-Ville distribution is a good candidate for our experimental data sets for analyzing micro-Doppler modulation due to its slightly reduced time-frequency resolution and largely reduced cross-term interference. However, other high-resolution time-frequency transforms also produce the same results in determining the motion parameters. The data analysis procedure is summarized in Table 1.

IV. Experimental Data

In this section we demonstrate examples of micro-Doppler signatures of targets that can be used as radar signatures for target identification. Experimental trials were conducted to investigate and resolve the micro-Doppler radar signatures of targets using an X-band radar. Two types of data collection were performed. The targets in these experiments are a helicopter and a walking man with swinging arms.

A. Helicopter Data

The experimental data used in the analysis that follows is of a hovering helicopter. For a helicopter, the main rotor blades, the tail rotor blades, and the hub have unique signatures suitable for target identification [9,26-27]. Generally, radar returns from a helicopter are back-scattered from the fuselage, the rotor blades, the tail blades, and the hub among other structures. The motion of the rotor blades depends upon the coupling between the aerodynamics and the rotor dynamics. Each blade is a rotating aerofoil having bending, flexing, and twisting motion. The radar cross section of a segment of the blade depends upon its distance from the centre of rotation, its angular position, and the aspect angle of the rotor [26]. For simplicity, the rotor blade can be modelled as a rigid, linear, and homogeneous rod rotating about a fixed axis with a constant rotation rate.

The rotational motion of rotor blades in a helicopter imparts a periodic modulation on radar returns. The rotation-induced Doppler shifts relative to the Doppler shift of the fuselage (or body) occupy unique locations in the frequency domain. Whenever a blade has specular reflection such as at the advancing or receding point of rotation, the particular blade transmits a short flash to the radar return. The rotation rate of the rotor is directly related to the time interval between these flashes. The duration of a flash is determined by the radar wavelength and by the length and rotation rate of the blades. A flash resulting from a blade with a longer length and a radar with a shorter wavelength will have a shorter duration [1].

The helicopter employed in the experiment is hovering above the ground at a height of approximately 60 m and at a range of 2.5 km from the radar. The main rotor is comprised of five blades and the tail rotor consists of six blades. The rotation rate of the main rotor blades is known to be 203 rpm for this helicopter. The rotation rate of the tail rotor blades is known to be 1030 rpm for this helicopter. The experiment was conducted using an X-band radar. Two trials were conducted, both with a time interval of 96.5 ms.

In order to demonstrate the procedure of m-D analysis, the results for trial 1 are now presented. First, the Fourier transform of the original radar returned data is computed and the image obtained is shown in Figure 2a. As can be seen from the image, a main frequency bin with a large amplitude exists in the middle of the spectrum representing the helicopter's body vibration. Surrounding this frequency bin, one can observe two other less promi-

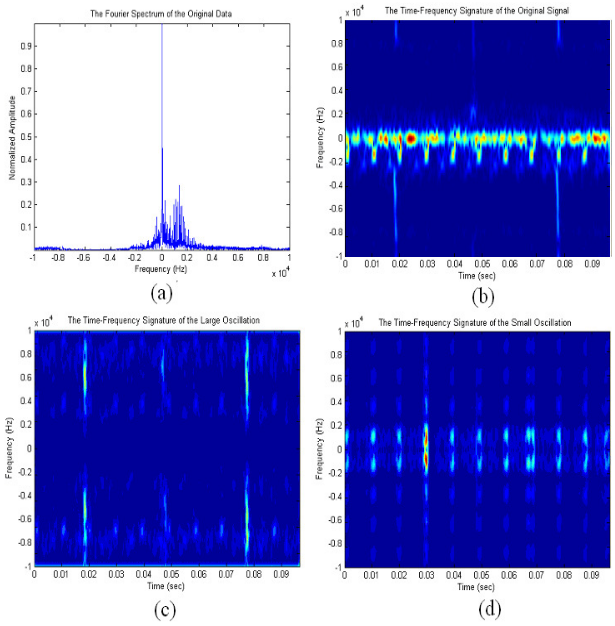

Fig. 2. (a) The Fourier spectrum of helicopter Trial 1; (b) The TF signature of the original data from helicopter Trial 1; (c) The TF signature of the extracted large oscillation from helicopter Trial 1; (d) The TF signature of the extracted small oscillation from helicopter Trial 1.

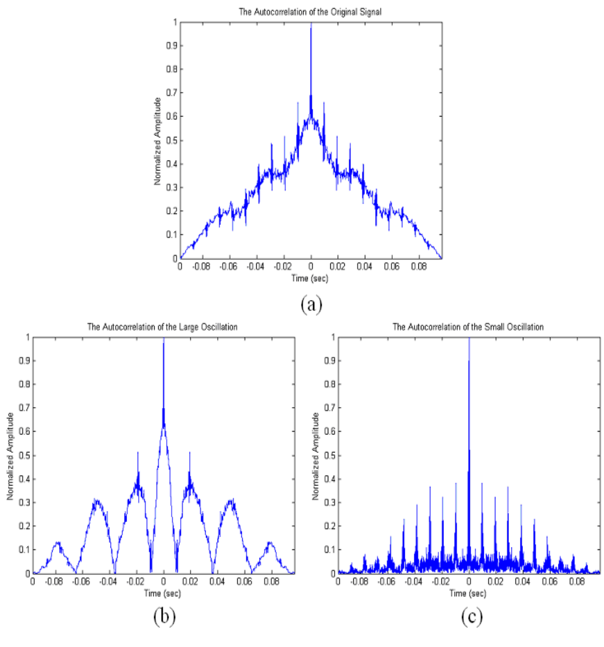

Fig. 3. (a) The autocorrelation of the original data from helicopter Trial 1; (b) The autocorrelation of the extracted large oscillation from helicopter Trial 1; (c) The autocorrelation of the extracted small oscillation from helicopter Trial 1.

TABLE I
Procedure for the radar m-D analysis.

Step 1.	Perform a 4 level decomposition of the signal s(t) using the db1 wavelet: s(t) $\rightarrow$ [ca_4, cd_1, cd_2, cd_3, cd_4].
Step 2.	Reconstruct the signal using coefficients from decomposition step 1: [ca_4, ca_1, ca_2, ca_3, ca_4] $\rightarrow$ [A_4, D_1, D_2, D_3, D_4].
Step 3.	Perform time-frequency analysis for selective component A_4 to get stationary target body.
Step 4.	Perform time-frequency analysis for selective components [D_3,D_4] to get large oscillation present in the signal.
Step 5.	Perform time-frequency analysis for selective components [D_1, D_2] to get small oscillation present in the signal.

nent peaks representing the frequency of the main rotor and tail rotor rotation rate. These are the m-D features that are to be extracted. By applying the wavelet analysis as described above, the m-D features are obtained. The next step in the procedure is to make use of time-frequency analysis in order to depict the m-D oscillations and to estimate the target's motion parameters. The time-frequency signature of the original returned signal using the smoothed pseudo Wigner-Ville distribution is given in Figure 2b. The stationary body is observed as a fairly constant signal at 0 Hz on the frequency axis. The micro-motion dynamics of the tail rotor are seen as small, quick flashes just below the constant stationary body. The micro-motions of the main rotor are visible as the three large flashes with the large period. The same time-frequency transform is applied to the extracted m-D feature representing the main rotor obtained from the wavelet analysis, and the resulting image is shown in Figure 2c. Here, not only are the flashes made clearer, but the flashes are in fact stronger peaks than those observed in the time-frequency signature of the original signal in Figure 2b. The rotation rate of the main rotor blades is calculated from Figure 2c as follows. It is known that the main rotor of this helicopter has five blades. This is an important point as it means that the specular reflection at the advancing and receding point of rotation do not coincide with one another. Therefore, the resulting time-frequency plot will show alternating strong and weak flashes. This is indeed the case in Figure 2c. The period between the two strong flashes, i.e. the period between two blades at the advancing point of rotation, is 0.0591 s. Since there are five blades, this value is multiplied by five in order to obtain 0.2955 s, the length of time taken by a single blade to complete one full rotation. The number of rotations in one minute is given by (60 s/min)/(0.2955 s/rotation) = 203.05 rpm, which is in agreement with the actual value known to be 203 rpm. Similarly, the smoothed pseudo Wigner-Ville distribution has been applied to the wavelet-extracted m-D feature representing the tail rotor. Figure 2d illustrates the end result. In this case, the flashes caused by the tail rotor have been made obvious by the removal of the stationary body and the main rotor components. Knowing that the tail rotor consists of six blades, the rotation rate of the tail rotor is measured using Figure 2d in a similar manner as it was computed for the main rotor. The rotation rate is calculated to be approximately 1031 rpm.

The rotation rate can also be estimated by taking the autocorrelation of the time sequence data of the extracted m-D features. The autocorrelation of the original signal is given in Figure 3a. It is evident that not much information can be easily extracted from this plot. However, looking at the plots of the autocorrelations for the extracted m-D features of the main rotor and tail rotor obtained using the wavelet decomposition method in Fig-

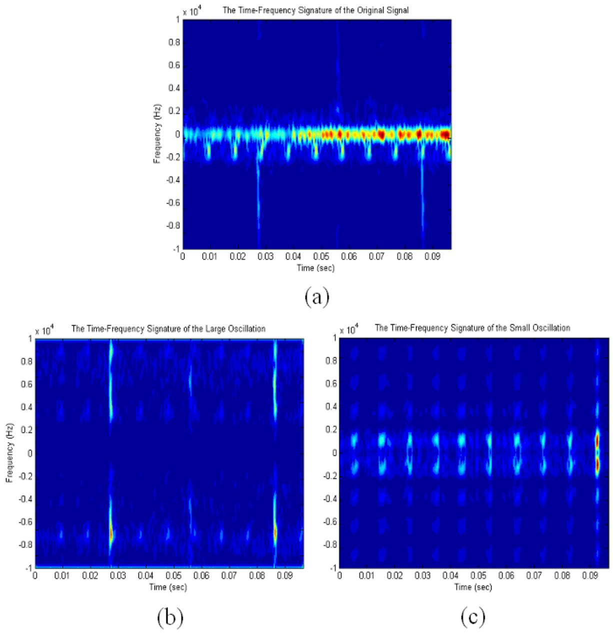

Fig. 4. (a) The TF signature of the original data from helicopter Trial 2; (b) The TF signature of the extracted large oscillation from helicopter Trial 2; (c) The TF signature of the extracted small oscillation from helicopter Trial 2.

ure 3b and Figure 3c, respectively, the oscillations are unmistakable. The distances between the peaks describe the period of the rotation, which in turn allows one to estimate the rotation rate. Using Figure 3b, the rotation rate of the main rotor blades is calculated to be 203 rpm, which is consistent with the value from the time-frequency analysis. Both results agree with the actual value. Note that without m-D extraction, it is more difficult to estimate the rotation rate from the autocorrelation of the original data as shown in Figure 3a. The peaks are much less prominent due to higher interference. The signal-to-noise ratio (SNR) is significantly enhanced after m-D extraction as compared to the original data.

Similar results are obtained in Trial 2. Figure 4a gives the time-frequency signature of the original radar returned data. Figure 4b shows the extracted m-D features representing the main rotor, while Figure 4c shows those representing the tail rotor. A scenario similar to Trial 1 is seen, where the plots after m-D extraction provide a much higher SNR and give clearer results. The rotation rate of the main rotor blades is calculated to be 203 rpm using the time-frequency plot of Figure 4b. The rotation of the tail rotor blades is calculated to be 1025 rpm.

B. Human Data

The human data used in this experiment was collected using the EARS (Experimental Array Radar System) employing a stepped frequency radar waveform [21,23]. The experiment was conducted with the radar operating at frequencies of 8.9 to 9.4 GHz, providing a 500 MHz bandwidth. The frequency step size was 10 MHz and a pulse repetition frequency (PRF) of 1 kHz was used. Thus, it required 50 ms to generate a single high-range resolution (HRR) profile (i.e. an effective HRR PRF of 20 Hz). The integration time for each data set was 60 seconds.

Experimental human data is used in the analysis that follows. The human gait is a complex motion that is comprised of the many movements of individual body parts. These moving body parts are the "structures" that exhibit unique m-D signatures suitable for target recognition. Hence, the information of interest contained in radar returns from human targets is the data representing the micro-motion dynamics of the various parts of the moving body. Since the body parts are moving at different velocities, a number of different frequency shifts will be obtained in the returned signal. Take, for example, a man walking and swinging his arms. The swinging motion of the arms may induce frequency modulation of the returned signal and generate sidebands about the body Doppler.

In particular, one would suspect that the motion of the swinging arms would cause a more prominent frequency modulation than the other components contributing to the radar returned signal due to the size and shape of the arms and the periodic nature of their motion in the walking gait. This being true, the experiment was conducted with an emphasis on the swinging motion of the human arms. The following 4 trials were conducted:

1) A human marching on the spot at 30 degrees to the radar, swinging two arms, with corner reflectors
2) A human marching on the spot at 60 degrees to the radar, swinging one arm, without a reflector
3) A human marching on the spot at 45 degrees to the radar, swinging two arms, without any reflectors

Note that the time interval for each trial was 60 seconds.

As the results obtained from the human gait experiments are acquired in a slightly different manner than those from the experimental helicopter data, the means by which the findings are attained must first be explained. The data from the radar returned signals for each trial are spread over a number of different 51 range cells. In order to proceed with the m-D analysis, a single range cell from the set of 51 must be selected so as to permit wavelet and time-frequency analysis. A range cell must be chosen that best represents the m-D feature that is being extracted. In this case, the desired m-D feature is the swinging arm. Thus, a range cell that captures the peaks of the arm swings (either the maximum or minimum points) should be selected so that the period of oscillation can be measured. Note that the period of oscillation of arm swings from all trials is known to be between 1.5 and 2.5 seconds. This is done deliberately in order to verify the results obtained from the experiments.

Now, the results of the experiment are presented starting with Trial 1 (the human marching on the spot and swinging two arms with reflectors). The image in Figure 5a shows the time series of the radar returned data. The image in Figure 5b shows a zoomed version of the time series over the time interval that will be considered in the m-D analysis. In a double arm swing, the frequency shift is seen as two oscillations, one from each arm, phase shifted from one another by half the period of the oscillation of one arm; this is assuming that the maximum amplitude (strong specular reflection) of the oscillation of one arm occurs at the same time as the weak specular reflection of the other arm (peak position of the arm behind the body). This is what is observed in the image of Figure 5b where a smaller, weaker, second oscillation is visible in the middle of the larger, stronger oscillation. The weaker oscillation represents the arm further away from the radar on the opposite side of the human body.

As described above, a range cell is selected in order to carry on with the wavelet analysis. In this case, range cell 30 is used, and the time-frequency signature of the resulting data using the smoothed pseudo Wigner-Ville distribution is given in Figure 5c. Range cell 30 is chosen because the maxima of the oscillations are all situated across that range, thereby allowing the oscillations to be represented by the six observed flashes in Figure 5c. By applying the wavelet analysis as described earlier, the m-D features of the signal at the selected range are obtained. Finally, time-frequency analysis is utilized in order to depict the m-D arm swing oscillations and to estimate the human gait motion parameters. The time-frequency signature of the extracted arm swing feature using the smoothed pseudo Wigner-Ville distribution is shown in Figure 5d. The period of the oscillation of the arm swing from the image

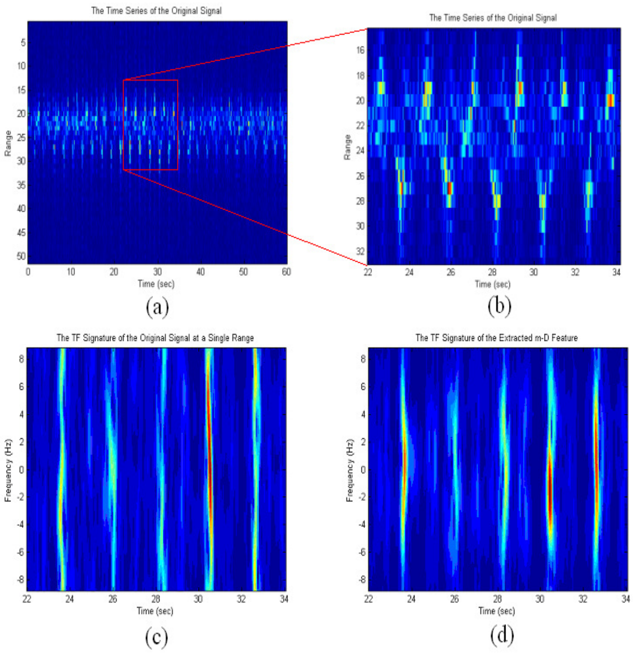

Fig. 5. (a) Time series of human Trial 1; (b) image shows the time interval under consideration for the m-D analysis; (c) TF signature at range cell 30; (d) TF signature after wavelet decomposition at range 30.

in Figure 5b is measured to be approximately 2.2 seconds. When the measurement is made using Figure 5c and Figure 5d separately, the same value of 2.2 seconds is obtained.

Trials 2 and 3 are analogous to Trail 1 except that they are both conducted without using any reflectors whatsoever. The images corresponding to Trial 2 (marching on the spot, one arm without reflector) are shown in Figures 6a, 6b, 6c, and 6d with range cell 19 having been selected. The time-series plot shown in Figure 6b reveals three distinguishable oscillations. Figure 6c gives the time-frequency signature of the signal obtained after selecting range cell 19 and the three oscillations are evident in the three strong flashes. However, the signal is much too noisy. Wavelet analysis is performed in order to extract the m-D features and the time-frequency signature of the resulting feature representing the arm swing is given in Figure 6d. Note the dramatic improvement of the SNR from Figure 6c to Figure 6d. Comparing Figures 6c and 6d, one observes a substantial decrease in noise after wavelet and time-frequency analysis. The reason is that during the reconstruction process of the detail levels, only the wavelet coefficients that are related to the m-D features (in this case arm swings) of the signal are used while other coefficients are set to zero. This process considerably "cleans up" the signal. Thereafter, when the time-frequency analysis is employed to analyse the arm swing oscillation, the results have higher precision after the m-D extraction since only arm swing components are employed. This procedure is different from traditional methods where the wavelet analysis and the time-frequency analysis are used independently. Here, we use the wavelet transform method combined with time-frequency analysis to extract m-D features. The period of the oscillation of the arm swings is measured to be 1.5 seconds from Figure 6b, from Figure 6c, and from Figure 6d.

Similarly, the images for Trial 3 (marching on the spot, two arms without any reflectors) are given in Figures 7a, 7b, 7c, and 7d. Here, the time interval under consideration includes six oscillations as is visible from the image in Figure 7b. Figure 7c gives the time-frequency

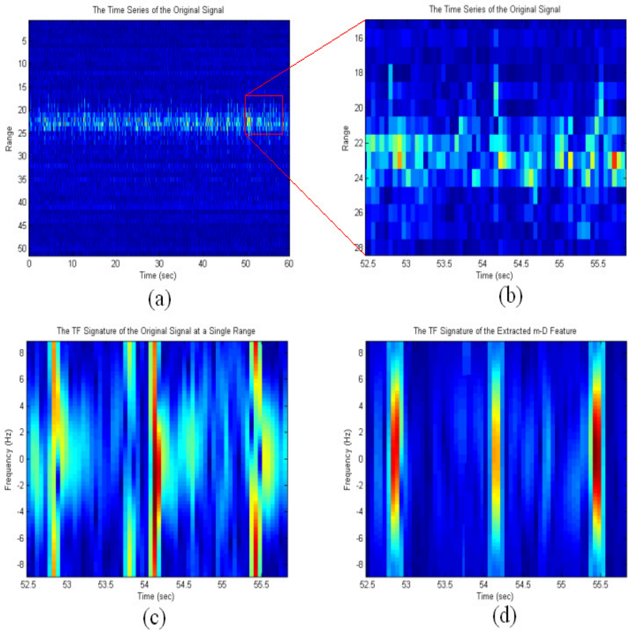

Fig. 6. (a) Time series of human Trial 2; (b) image shows the time interval under consideration for the m-D analysis; (c) TF signature at range cell 19; (c) TF signature after wavelet decomposition at range 19.

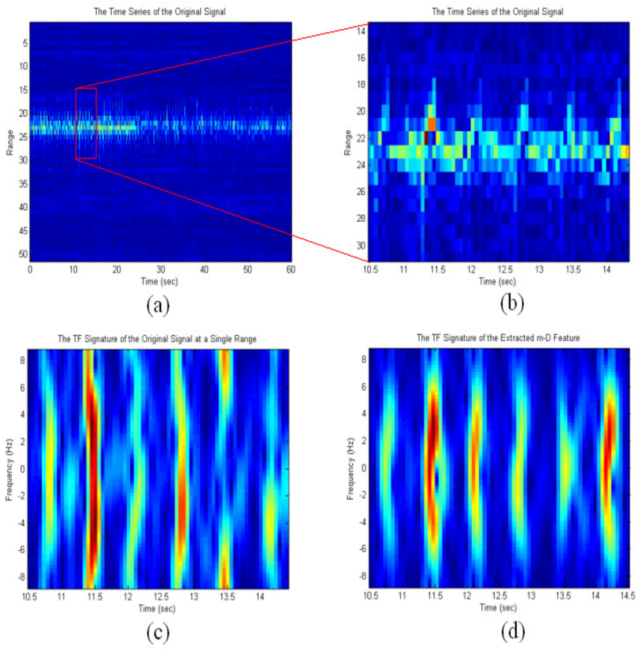

Fig. 7. (a) Time series of human Trial 3; (b) image shows the time interval under consideration for the m-D analysis; (b) TF signature at range cell 20; (c) TF signature after wavelet decomposition at range 20.

representation of the data at range cell 20. Again, wavelet analysis is performed in order to extract the m-D feature indicating the motion of the arm swing, and the time-frequency signature of the feature is shown in Figure 7d. One can see that there exists much less background noise in this image than that of the original signal given in Figure 7c. The six flashes representing the six oscillations are clearly identifiable in this image. Keeping in mind that this trial includes two arms swinging, the period of oscillation of the arm swings is measured to be 1.5 seconds from Figure 7b, from Figure 7c, and from Figure 7d.

We can see that the body's Doppler shift is almost constant but the arm's micro-Doppler shift becomes time-varying and has an oscillation. All of the results demonstrate that the m-D features are made substantially clearer after m-D analysis has taken place and establish that the period of oscillation of the arm swings is completely verified. These results show that the radar gait image analysis integrated with m-D can provide new identification methods for remote detection of walking personnel either in battlefield or urban scenarios, dealing with hostage acts, detecting humans (soldiers) in a forest, through wall human detection, search and rescue scenarios, perimeter protection, border monitoring etc.

V. Conclusion

This paper presents a procedure for m-D analysis in order to extract the m-D features of radar returned signals from targets. The method combines both wavelet and time-frequency analysis in order to extract the m-D features of radar target returns. By applying the proposed procedure to helicopter and human gait data, the effectiveness of this analysis technique is confirmed. From the extracted m-D signatures, information about the target's micro-motion dynamics, such as rotation rate and period of oscillation, has been obtained.

The wavelet transform method is applied during the m-D analysis process in order to extract m-D features from radar returns. The various signal components are obtained at different wavelet scales in the decomposition process. The extraction of m-D features is completed by the reconstruction process in which the inverse wavelet transform is applied. This methodology has been applied to helicopter data with rotational motion and human gait data. The results show that the wavelet transform methodology is an effective tool for extracting m-D features. After the extraction of m-D features, time-frequency analysis is employed in order to depict the oscillation and estimate the motion parameters. The rotation rates of the main rotor and tail rotor blades of the helicopter are successfully computed as are the periods of oscillation of the arm swings of the human gait. The vibration/rotation rate of the helicopter is also estimated by taking the autocorrelation of the time sequence data. In general, it is shown that the results are much improved after the m-D extraction has taken place since only the vibrational/rotational components are employed. The experimental results agree with the expected outcome. In a future study, we intend to develop a new adaptive time-frequency and scale transform for feature extraction and recognition purpose.

The detection and extraction of m-D features in radars is still immature. No known comprehensive model of the m-D phenomenon applied to radar exists in open literature. The analysis of m-D detection and extraction using time-frequency techniques or wavelets is relatively new and has to be explored further. The current decomposition methods are not designed to fully represent "deep level" information from radar signatures such as the m-D effect, which affects radar Automatic Target Recognition (ATR), especially for weak moving targets buried in noise and target returns with strong vibration or rotational components. These methods are not designed to deal with a variety of targets of interest and often do not offer the flexibility of selective feature composition during the reconstruction process (i.e. inverse transform). Therefore new algorithms, adaptive transforms and methods will be investigated in the future to address these issues.

References

[1] Chen, V.C. and Ling, H. (2002). Time-Frequency transform for radar imaging and signal analysis, *Artech House,* BOSTON.

[2] Chen, V. C. (2000). Analysis of Radar Micro-Doppler Signature with Time Frequency Transform, *Proc. Tenth IEEE Workshop on Statistical Signal and Array Processing,* pp. 463-466.

[3] Li, J., and Ling, H. (2003). Application of adaptive chirplet representation for ISAR feature extraction from targets with rotating parts, *IEE Proc-Radar Sonar Navig.,* Vol. 150, No. 4, pp. 284-291.

[4] Sparr, T., and Krane, B. (2003). Micro-Doppler analysis of vibrating targets in SAR, *IEE Proc-Radar Sonar Navig.,* Vol. 150, No. 4, pp. 277-283.

[5] Thayaparan, T. (2004). Micro-Doppler radar signatures for intelligent target recognition, *DRDC Ottawa TM 2004-170,* Defence R&D Canada - Ottawa.

[6] Thayaparan, T. and Abrol, S., Micro-Doppler Analysis of Rotating Target in SAR, DRDC Ottawa TM 2005-204, December 2005, 43 pages.

[7] Chen, V. C., Li, F., Ho, S.-S., and Wechsler, H, Micro-Doppler effect in radar: phenomenon, model, and simulation study, Vol. 42, No. 1, pp. 2-21, *IEEE Trans. on Aerospace and Electronis Systems,*, 2006.

[8] Greneker, G., Geisheimer, J., and Asbell, D., "Extraction of Micro-Doppler from Vehicle Target at X-band Frequency,' Proceeding of SPIE on Radar Technology, Vol. 4374, 2001.

[9] Wellman, R.J., and Silvious, J. L. (1998). Doppler Signature Measurements of an Mi-24 Hind-D Helicopter at 92 GHz, ARL-TR-1637, *Army Research Laboratory,* Adelphi, Maryland.

[10] Bell, M. R., and Grubbs, R. A. (1993). JEM Modeling and Measurement for Radar Target Identification, *IEEE Trans. Aerospace Electron. Syst.,* Vol. 29, pp.73-87.

[11] Sommer, H. and Salerno, J. (1971). Radar Target Identification System, U.S. Patent 3, pp. 614,779.

[12] Tremblay, F. (1995). Generalization of the DREO radar jet engine modulation algorithm, DREO TR 1995-1199.

[13] van Dorp, P., and Groen, F. C. A. (2003). Human walking estimation with radar", *IEE Proc-Radar Sonar Navig.,* Vol. 150, No. 5.

[14] Geisheimer, J. L., Greneker, E. F., and Marshall, W. S., A High-Resolution Doppler Model of Human Gait, Georgia Tech Research Institute, 7220 Richardson Rd., Smyrna, GA 30080.

[15] Little, J.J. and Boyd, J. E. (1998). Recognizing people by their gait: the shape of motion, *Journal of Computer Vision Research,* vol. 1, no. 2.

[16] Niyogi, S. A. and Adelson, E. H. (1994). Analyzing and recognizing walking figures in XYT, *IEEE Proceedings on Computer Vision and Pattern Recognition,* pp. 469-474.

[17] Sabatini, A. M. and Colla, V. (1998). A method for sonar based recognition of walking people, *Robotics and Autonomous Systems,* Vol. 24, pp. 117-126.

[18] Weir, R. F. and Childress, D. S. (1997). A new method of characterizing gait using a potable, real-time, ultrasound ranging device, *Proceedings of the 19th International Conference,* IEEE Engineering in Medicine and Biology Society, pp. 1810-1812.

[19] Yasotharan, A. and Thayaparan, T. (2002). Strengths and limitations of the Fourier method for detecting accelerating targets by pulse Doppler radar, *IEE Proc.-Radar Sonar Navig.,* Vol 149, No. 2, pp 83-88.

[20] Cohen, L. (1995). Time-frequency analysis, Prentice Hall PTR, New Jersey.

[21] Thayaparan, T., Lampropoulos, G., Wong, S. K. and Riseborough, E. (2003). Application of adaptive time-frequency algorithm for focusing distorted ISAR images from simulated and measured radar data, *IEE Proc.-Radar Sonar Navig.,* Vol. 150, No. 4, pp. 213-220.

[22] Thayaparan, T. and Kennedy, S. (2004). Detection of a maneuvering air target in sea-clutter using joint time-frequency analysis techniques, *IEE Proc.-Radar Sonar Navig.,* Vol. 151, No. 1, pp. 11-18.

[23] Lampropoulos, G., Thayaparan, T., and Xie, N., Fusion of time-frequency distributions and applications to radar signals, *Journal of Electronic Imaging,* 15(2), pp. 1-17, 2006.

[24] Mallat, S. (1989). A theory for multiresolution signal decomposition: The wavelet representation, *IEEE Trans. Pattern Anal. Machine Intell.,* Vol. 11, pp. 674-693.

[25] Misiti, M., Misiti., Y., Oppenheim, G., and Poggi, J.-M. (2002). Wavelet Toolbox, *The MathWorks Inc.,* Natick, MA, USA,

[26] Martin, J. and Mulgrew, B. (1990). Analysis of theoretical radar return signal from aircraft propeller blades, *IEEE 1990 international radar conference,* pp. 569-572.

[27] Marple, S. L. (2001). Large dynamics range time-frequency signal analysis with application to helicopter Doppler radar data, *ISPA Conference,*